PHYSICAL REVIEW E VOLUME 62, NUMBER 3 SEPTEMBER 2000

Asymmetric squares as standing waves in Rayleigh-Bénard convection

Alaka Das, Ujjal Ghosal, and Krishna Kumar
Physics and Applied Mathematics Unit, Indian Statistical Institute, 203 Barrackpore Trunk Road, Calcutta 700 035, India
(Received 26 October 1999)

Possibility of thermal convection in the form of asymmetric squares in a thin layer of Boussinesq fluids of large lateral extension confined between stress-free and conducting flat boundaries is investigated numerically using a seven mode Lorenz-like model. For fluids with moderate and high Prandtl numbers ($4<\sigma<20$) and in a narrow window of high Rayleigh numbers ($12<R/R_c<15$), which depend on Prandtl number, the stationary rolls become unstable and asymmetric squares appear as standing waves at the onset of secondary instability. Asymmetric squares, two-dimensional rolls, and again asymmetric squares with their corners shifted by half a wavelength form a stable limit cycle. The oscillatory bifurcation is supercritical.

PACS number(s): 47.20.Ky, 47.27.−i

Two-dimensional stationary roll patterns are known to be the only stable solutions at the onset of thermal convection in a thin layer of Boussinesq fluid confined between conducting boundaries [1], except in the case of fluids with vanishingly small Prandtl number [2]. The stationary convection in the form of symmetric square cells are unstable [1] except in fluids of high Prandtl number ($\sigma>10$) at very high values of Rayleigh number R [3]. Assenheimer and Steinberg [4] observed an interesting possibility of hexagonal convective cells with both up and down flow in the center of the cell at R approximately twice the value of critical Rayleigh number R_c. The possibility of dual types of hexagonal convective cells was also established by Clever and Busse [5]. Recently, Busse and Clever [6] predicted the possibility of stationary convection in the form of asymmetric square cells with both up and down flow in the center at high Rayleigh numbers ($3.5<R/R_c<15.7$) in a Boussinesq fluid ($\sigma=7$) confined between rigid and thermally conducting horizontal boundaries. The asymmetry in square cells was observed in vertical plane.

In this Rapid Communication, we present a theoretical study of the possibility of asymmetric squares as convective cells in ordinary fluids in Rayleigh-Bénard geometry. We are interested in asymmetry in horizontal layers of fluid rather than in vertical layers as studied by Busse and Clever [6]. We construct and study a minimum mode Lorenz-like model [7] that describes convection patterns in the form of rolls and squares, both symmetric as well as asymmetric ones, in a thin layer of Boussinesq fluid of moderate and high Prandtl numbers ($4<\sigma<20$). The nonlinear superposition of mutually perpendicular sets of rolls of the same wave number would be called asymmetric squares when the structure (e.g., shadowgraph picture) does not possess fourfold symmetry. It happens when the intensities of the two sets of rolls are different. The model allows us to study any possible competetion between rolls and asymmetric squares. In the following we shall derive the model from hydrodynamic equations and investigate the model numerically for possible stable solutions. We then present the results and discuss them.

We consider an infinite layer of Boussinesq fluid of kinematic viscosity ν, thermal diffusitivity κ, and thickness d confined between two perfectly conducting horizontal boundaries and heated underneath. Using the thickness d of the fluid layer as length scale, the thermal diffusive time ($=d^2/\kappa$) as the time scale, and the temperature difference ΔT between lower and upper flat boundaries as the temperature scale, the nondimensional form of relevant hydrodynamic equations in Boussinesq approximation reads

$$\partial_t \nabla^2 v_3 = \sigma \nabla^4 v_3 + \sigma \nabla_H^2 \theta - \mathbf{e}_3 \cdot \boldsymbol{\nabla} \times [(\boldsymbol{\omega} \cdot \boldsymbol{\nabla})\mathbf{v} - (\mathbf{v} \cdot \boldsymbol{\nabla})\boldsymbol{\omega}], \tag{1}$$

$$\boldsymbol{\nabla} \cdot \mathbf{v} = 0, \tag{2}$$

$$\partial_t \theta = \nabla^2 \theta + R \mathbf{v} \cdot \mathbf{e}_3 - \mathbf{v} \cdot \boldsymbol{\nabla} \theta, \tag{3}$$

where $\mathbf{v}=(v_1,v_2,v_3)$ are the velocity fields, θ the deviation from the conductive temperature profile, and p the deviation from static pressure of conductive state due to convective instability. $\boldsymbol{\omega}=\boldsymbol{\nabla}\times\mathbf{v}$ is the vorticity, and $\nabla_H^2=\partial_{11}+\partial_{22}$ is the horizontal Laplacian. Equation (1) is obtained by taking curl twice of the momentum equation and using the continuity condition [Eq. (2)]. Prandtl number σ and Rayleigh number R are defined as $\sigma=\nu/\kappa$ and $R=[\alpha(\Delta T)g d^3]/\nu\kappa$, where α is the coefficient of thermal expansion of the fluid, and g the acceleration due to gravity. The unit vector $\mathbf{e}_3$ is directed vertically upward, which is assumed to be the positive direction of x_3 axis. The boundary conditions at the stress-free conducting flat surfaces imply $\theta=v_3=\partial_{33}v_3=0$ at $x_3=0,1$.

We employ the standard Galerkin procedure to describe the convection patterns at the onset of secondary instability in fluids with Prandtl number $\sigma>4$. The spatial dependence of all vertical velocity and temperature field are expanded in a Fourier series, which is compatible with the stress-free flat conducting boundaries and periodic boundary conditions in the horizontal plane. As we are interested in studying square cell convection, we restrict ourselves to standing patterns and, hence all time-dependent Fourier amplitudes will be assumed to be real. The expansions for all the fields are truncated to describe straight cylindrical rolls and patterns arising from the nonlinear superposition of mutually perpendicular set of rolls of the same wave to number. Perturbative fields with the same wavelength in mutually perpendicular directions are likely to occur in small aspect ratio square containers. The vertical velocity v_3 and θ then read as

$$v_3=[W_{101}(t)\cos kx_1+W_{011}(t)\cos kx_2]\sin \pi x_3 + W_{112}(t)\cos kx_1\cos kx_2\sin 2\pi x_3, \quad (4)$$

$$\theta=[\Theta_{101}(t)\cos kx_1+\Theta_{011}(t)\cos kx_2]\sin \pi x_3 + \Theta_{112}(t)\cos kx_1\cos kx_2\sin 2\pi x_3+\Theta_{002}(t)\sin 2\pi x_3. \quad (5)$$

The horizontal components of the velocity field can easily be computed using the equation of continuity. Projecting Eq. (4) for v_3 and the equation for θ [Eq. (3)] on above modes, we arrive at the following seven mode Lorenz-like model

$$\tau\dot{\mathbf{X}}=\sigma[-\hat{q}^2\mathbf{X}+(\hat{k}^2/\hat{q}^2)\mathbf{Y}]+(X_2,X_1)^{\mathrm{T}}\ S, \quad (6)$$

$$\tau\dot{\mathbf{Y}}=-\hat{q}^2\mathbf{Y}+(r-Z)\mathbf{X}+(X_2,X_1)^{\mathrm{T}}\ T, \quad (7)$$

$$\tau\dot{S}=-2\sigma\hat{d}^2S+\sigma(\hat{k}^2/\hat{d}^2)T-(\hat{q}^2/2\hat{d}^2)X_1X_2, \quad (8)$$

$$\tau\dot{T}=-2\hat{d}^2T+rS-(X_1Y_2+X_2Y_1)/4, \quad (9)$$

$$\tau\dot{Z}=-bZ+\mathbf{X}\cdot\mathbf{Y}, \quad (10)$$

where the linear modes

$$\mathbf{X}\equiv(X_1,X_2)^{\mathrm{T}}=\pi/\sqrt{2}q_c^2(W_{101},W_{011})^{\mathrm{T}}$$

and

$$\mathbf{Y}\equiv(Y_1,Y_2)^{\mathrm{T}}=\pi k_c^2/\sqrt{2}q_c^6(\Theta_{101},\Theta_{011})^{\mathrm{T}}$$

represent the vertical velocity and the temperature field respectively. The nonlinear mode $Z=(-\pi k_c^2/q_c^6)\Theta_{002}$ denotes heat flux across the fluid layer. Modes $S=(\pi/4q_c^2)W_{112}$ and $T=(\pi k_c^2/4q_c^6)\Theta_{112}$ are essential to describe nonlinear coupling between two sets of mutually perpendicular rolls. The model, thus, consists of minimum numbers of modes required to describe straight rolls and squares. The parameters defined by $q^2=\pi^2+k^2$, $\hat{q}^2=q^2/q_c^2$, $\hat{k}^2=k^2/k_c^2$, and $\hat{d}^2=(2\pi^2+k^2)/q_c^2$ are, in general, wave number dependent, while other parameters given by $k_c^2=\pi^2/2$, $q_c^2=\pi^2+k_c^2$, $\tau=1/q_c^2$, and $b=4\pi^2/q_c^2$ are constants in the model. The reduced Rayleigh number $r=Rk_c^2/q_c^6$ is the control parameter of the problem. We set, hereafter, $k=k_c$, the wave number of stationary rolls at the onset of primary instability. This makes $\hat{k}^2=\hat{q}^2=1$, $\hat{d}^2=\frac{5}{3}$ and $b=\frac{8}{3}$ in our model for convection.

The steady two-dimensional (2D) rolls parallel to the x_1 axis are given by $X_1=0=Y_1$. This makes the nonlinear modes S and T decouple from the system. Our model then reduces to well known Lorenz model with steady solutions given by $X_2=Y_2=\sqrt{b(r-1)}$ and $Z=r-1$. However, these solutions become unstable at much lower values of reduced Rayleigh number r than that predicted by the original Lorenz model [7]. The lower curve in Fig. 1 shows the critical value r_o of reduced Rayleigh number, at which the 2D rolls become unstable, as a function of the Prandtl number σ. The critical value r_o increases with increasing σ. The steady and perfect squares are obtained by setting $X_1^2=X_2^2$ in our model.

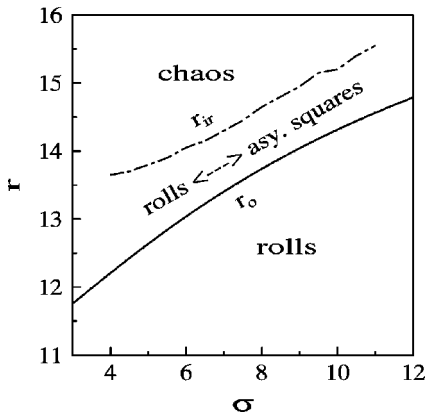

FIG. 1. Region of r and σ space showing rolls, asymmetric squares, and irregular solutions. The lower curve shows the values of reduced Rayleigh number r_o above which 2D rolls become unstable and time periodic asymmetric squares appear. The upper curve corresponds to the onset of chaotic solutions in the model.

Such solutions exist in our model, which is valid for $1<r<r_o(<4\hat{d}^2)$. However, they are found to be always unstable.

We study the time-dependent solutions by numerically integrating our model. We investigate the dynamics of the patterns as a function of increasing r in two ways: first by using the data from previous solution as initial conditions for a new r, and second by choosing randomly small values of all variables as initial conditions. We get the same result with suitably chosen initial conditions. For $r_o<r<r_{ir}$ (see Fig. 1), we find oscillatory solutions. The stationary rolls become unstable and a new set of rolls perpendicular of the old one develops as r is raised above r_0. The competition between these two sets of rolls leads to a time periodic sequence of rolls and patterns arising from nonlinear superposition of two sets of rolls. For $r>r_{ir}$, the solutions of the model become irregular, indicating more modes may be required to study this regime of parameter space. Higher order modes in the horizontal plane may distort the pattern without contributing significantly to the transport of heat across the fluid layer.

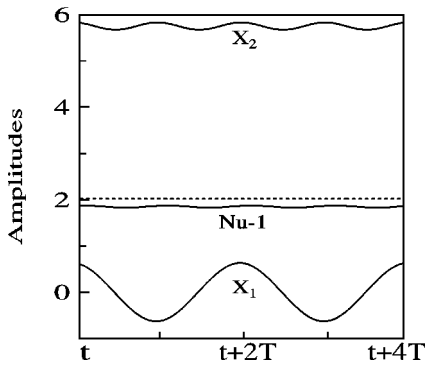

FIG. 2. Convective amplitudes X_2 (the uppermost curve) and X_1 (the lowermost curve) of new and old sets of rolls respectively with respect to time for $r=13.5$ and $\sigma=7$. The time period of the new set of rolls is always double that for the old set of rolls, which became stable. The Nusselt number of the model (solid curve in the middle) shows the oscillating behavior and its mean value is within 8% of the Nusselt number reported by direct simulation (dotted line) of Busse and Clever [6] with ''no-slip'' conditions.

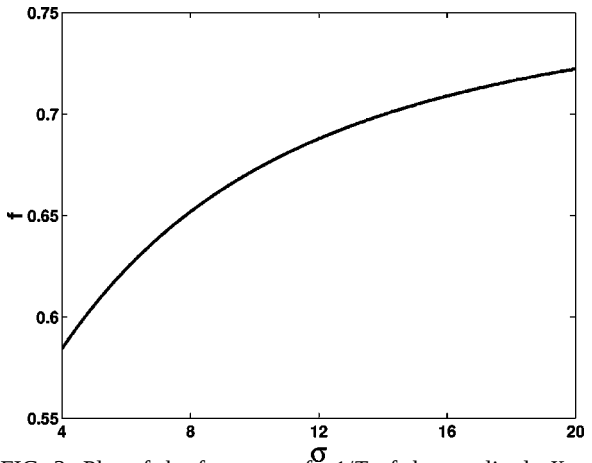

FIG. 3. Plot of the frequency $f=1/T$ of the amplitude X_2 as a function of Prandtl number σ at the onset of secondary instability.

Our simple model does not include higher order modes, which might be essential as r is raised much above r_0. This may be the cause of irregular behavior at higher values of r.

Figure 2 shows the temporal behavior of the amplitude X_1 of the new set of rolls as well as the amplitude X_2 of the old set of rolls. While X_1 oscillates with zero mean, X_2 oscillates around a finite value. The time period of X_1 is always double of that of X_2. In fact, all the modes (X_1, Y_1, S, T) that develop at $r>r_o$ oscillate with same period and with zero mean. The periods of Y_2 and Z are the same as that of X_2. The Nusselt number (the solid curve in the middle) predicted by the seven mode model is also compared with that of the same obtained by direct numerical simulation for Boussinsq fluids confined between two flat rigid boundaries in Fig. 2. The mean of the Nusselt number of the seven mode model is within 8% of the Nusselt number (dotted line) obtained by direct numerical simulation of Ref. [6] for $\sigma=7$.

The periodic solution arises via supercritical Hopf bifurcation with amplitude of the oscillating mode with nonzero mean (e.g., X_2) scales as $\sqrt{(r-r_0)}$. The frequency of oscillation is finite at the onset of secondary instability. The frequency $f=1/T$ of oscillation of the mode X_2 at the onset of oscillatory instability increases with increasing Prandtl number (see Fig. 3). The mean of oscillating amplitude of 2D roll mode (X_2) decreases and the perturbative amplitude (X_1) increases with increasing r. Figure 4 shows two shadowgraphs of the standing wave patterns in the form of asymmetric squares for $r_o<r<r_{ir}$. The intensity of old 2D rolls decreases when a new set of rolls perpendicular to the old one appears. While the spatial positions for up and down flows in the old set remain fixed, these positions alternate for new set of rolls. Consequently, the corner positions of square patterns slide back and forth along the set of old rolls. The standing waves in form of square patterns do not have fourfold symmetry, although they preserve inversion symmetry. The time periodic appearances of asymmetric squares, 2D rolls, asymmetric squares again with shifted positions of the maximum up or down flows by half a wavelength, and 2D rolls form a limit cycle. Although the competetion between rolls and symmetric squares is known in binary mixtures [8, 9], the time periodic sequence of asymmetric squares and two-dimensional rolls in pure fluids is qualitatively new.

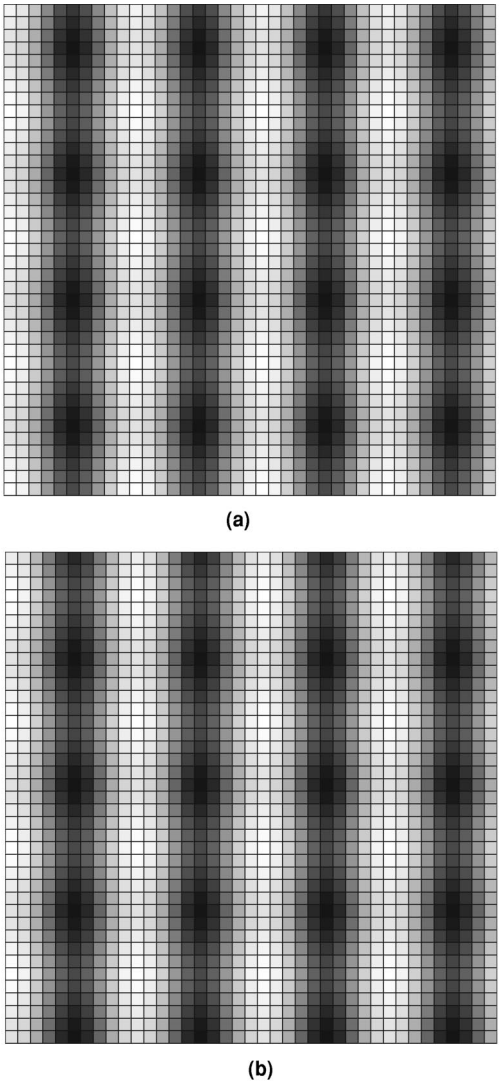

FIG. 4. Shadowgraphs of asymmetric squares at time t and $t+T/2$ for $r=14.7$ and $\sigma=10$.

We now test the stability of this limit cycle by introducing the vertical vorticity in the model. We expand the vertical vorticity ω_3 in Fourier modes ζ_{101}, ζ_{011}, and ζ_{110}. Simultaneously, for the consistency of the model, we add a mode $W_{\overline{112}}$ in the expansion of vertical velocity v_3, and a similar mode $\Theta_{\overline{112}}$ in the expansion of temperature field θ. This makes a Lorenz-like model consisting of twelve modes. The results of this model for fluids with $\sigma>4$ exactly reproduces the results of the seven mode model discussed earlier. For $\sigma<2$, vertical vorticity is excited at the onset of secondary instability. For $\sigma>4$ and perturbations of wave number same as that of 2D rolls, we always see a stable limit cycle. We have also checked the results for test cases for $\sigma=10$ by direct numerical simulation of 3D Boussinesq equations for the case of free-slip boundary conditions. This is done by using Galerkin technique with wave number set equal to k_c. The spatial resolution is chosen compatible with low aspect ratio containers. The results of two methods are in good agreement for values or r just above the onset of secondary instabilities (i.e., above the solid curve of Fig. 1). The mean of Nusselt number predicted by the model is within 8% of the same obtained from the simulation. Many higher order

modes develop as r is raised much above r_o without changing the mean Nusselt number significantly for the test cases. The results of our model indicates that for moderate and high Prandtl number fluids ($4<\sigma<20$) enclosed preferably in a small aspect ratio square container, the time periodic competition between the asymmetric squares and rolls may be realizable close to the onset of secondary instability in a narrow range of relatively high Rayleigh numbers ($12<r<15$). The range of Rayleigh numbers depends on the Prandtl number of the fluid. In addition, the model represents a simple dynamical system to study competetion between asymmertic squares and straight rolls.

We acknowledge support from DST, India. Ujjal Ghosal, from IIT, Kharagpur, acknowledges partial support from ISI, Calcutta.

[1] A. Schlüter, D. Lortz, and F. Busse, J. Fluid Mech. **23**, 129 (1965).
[2] O. Thual, J. Fluid Mech. **240**, 229 (1992); see also K. Kumar, S. Fauve, and O. Thual, J. Phys. II **6**, 945 (1996).
[3] J.A. Whitehead and B. Parsons, Geophys. Astrophys. Fluid Dyn. **9**, 201 (1978).
[4] M. Assenheimer and V. Steinberg, Phys. Rev. Lett. **76**, 756 (1996).
[5] R.M. Clever and F.H. Busse, Phys. Rev. E **53**, R2037 (1996).
[6] F.H. Busse and R.M. Clever, Phys. Rev. Lett. **81**, 341 (1998).
[7] E.N. Lorenz, J. Atmos. Sci. **20**, 130 (1963).
[8] E. Moses and V. Steinberg, Phys. Rev. Lett. **57**, 2018 (1986).
[9] H.W. Müller and M. Lücke, Phys. Rev. A **38**, 2965 (1988).